

## Thyrotropin receptor autoantibody (TRAb) enhance the expression of thyrotropin receptor on mouse brain vascular endothelial cells: in vivo and in vitro

Chunfeng Liang<sup>1</sup>, Haiyan Yang<sup>2</sup>, Xuemei Huang<sup>2</sup>, Yaqi Kuang<sup>2</sup>, Xiujun Deng<sup>2</sup>, Yuping Liu<sup>2</sup>, Zuojie Luo<sup>2\*</sup>

<sup>1</sup>Department of Blood Transfusion, The First Affiliated Hospital of Guangxi Medical University, Nanning, 530021, China

<sup>2</sup>Department of Endocrinology, The First Affiliated Hospital of Guangxi Medical University, Nanning, 530021, China

### ARTICLE INFO

#### Original paper

#### Article history:

Received: August 17, 2023

Accepted: September 19, 2023

Published: September 30, 2023

#### Keywords:

Acute hyperthyroid myopathy, BEnd.3 cells, Graves' disease, Thyrotropin receptor, Thyrotropin receptor autoantibody

### ABSTRACT

The possibility that thyrotropin receptor (TSHR) expression in non-thyroid tissue is well-documented. However, there is insufficient data on the expression of TSHR in medulla oblongata regions, particularly when focusing on the background of encephalopathy associated with hyperthyroidism. In this study, we explored the expression of the functional TSHR in Graves' disease (GD) mouse cerebral vascular endothelial cells and the effects of thyrotropin receptor autoantibody (TRAb) on its expression. A mouse model of GD was constructed with an adenovirus overexpressing TSHR289. The location and expression of the TSHR gene and protein in vivo were determined via RT-qPCR, Western blot, and immunofluorescence techniques. The effect of TRAb on the expression of functional TSHR in vitro was investigated using bEnd.3 cells. Our results show that medulla oblongata vascular endothelial cells from GD mice expressed higher levels of TSHR compared to control mice. In an in vitro experiment, novel results demonstrated that after treatment with a monoclonal TSHR-specific agonistic antibody (M22), the expression of TSHR on the bEnd.3 cells increased at both the protein and mRNA levels. Furthermore, compared with bEnd.3 cells were treated with IBMX only, those treated with M22 showed increased cAMP production. This study suggested that TSHR is expressed and functionally active in the mouse medulla oblongata and in vitro-cultured bEnd.3 cells and TRAb (M22) increased the expression of TSHR on bEnd.3 cells.

Doi: <http://dx.doi.org/10.14715/cmb/2023.69.9.10>

Copyright: © 2023 by the C.M.B. Association. All rights reserved.

### Introduction

Acute thyrotoxic myopathy (ATM) is also known as acute hyperthyroidism bulbar paralysis, it is a rare, severe, and rapidly progressive complication of hyperthyroidism, which is characterized by weakness of the muscle groups innervated by medulla oblongata (1). Although encephalopathy associated with ATM has been described several decades ago (2-5), due to the inaccessibility of the brain, it is difficult to obtain corresponding brain samples at the time of ATM onset, this association is still not well defined. Notably, Waldenstrom et al. 's autopsy findings indicate that there was hemorrhage into the medulla oblongata nerve nuclei and around the vagal nucleus in the bottom of the fourth ventricle for 3 cases with ATM (6). Hyperthyroidism can potentially cause encephalopathy, according to Chapman and Maloof (7). They discovered swelling of oligodendroglia in the subcortical white matter after doing a microscopic brain exam.

Graves' disease (GD) as the most common cause of hyperthyroidism (8), thyrotropin receptor (TSHR) autoantibodies (TRAbs), is the main pathogenic autoimmune antibodies, target TSHR, which is an important cause of hyperthyroidism in GD (9-11). Besides, in addition to being expressed in thyrocytes, TSHR is also expressed in extra-thyroid organs, such as the anterior pituitary gland and hypothalamus (12). We speculate that there is a common antigen in the medulla oblongata and thyroid tissue, TSHR is a target of the cellular autoimmune response.

High concentrations of TRAbs in the blood of patients with GD may affect the expression of TSHR in medulla oblongata vascular endothelial cells and thyrotropin receptor distribution in the brain may involved in the development of bulbar dysfunction.

In this study, we established a TRAb-positive BALB/c mouse model of GD with a TSHR-expressing adenovirus to study the presence and cellular localization of TSHR in the mouse medulla oblongata and used a monoclonal TSHR-specific stimulating antibody (M22) to simulate different concentrations of TRAbs in vitro to determine whether and how different concentrations of TRAbs affect the expression of TSHR on the surface of mouse brain endothelial (bEnd.3) cells.

### Materials and Methods

#### Mice

The Vital River Laboratory Animal Technology Co., Ltd. (Beijing, China) provided us with female BALB/c mice aged 6 weeks. Protocols authorized by The Animal Care and Welfare Committee of Guangxi Medical University (Guangxi, China) were adopted in all animal studies. Throughout the research, mice were housed in specific pathogen-free conditions.

#### Immunization of mice with a TSHR A-subunit-expressing adenovirus

To induce the occurrence of GD, we used the adenovi-

\* Corresponding author. Email: [luozuojie@gxmu.edu.cn](mailto:luozuojie@gxmu.edu.cn)

rus immunization method to inject mice with recombinant adenovirus overexpressing the TSHR-A subunit (13). In this study, all mice were divided into 3 groups, and the Ad-Control group was used as a negative control. The mice in the blank control group were intramuscularly (i.m.) injected with 100  $\mu$ l of phosphate-buffered saline (PBS) (n=6), those in the Ad-Control group were i.m. injected with 100  $\mu$ l of PBS containing  $5.7 \times 10^7$  PFU of Null-TSHR289 (n=6), and those in the GD group were i.m. injected with 100  $\mu$ l of PBS containing  $5.7 \times 10^7$  PFU of Ad-TSHR289 (n=6). The recombinant adenovirus expressing TSHR289 was constructed by Shanghai GeneChem Co., Ltd. Three injections were given to each animal at three-week intervals. The mice were sacrificed four weeks following their final immunization, and their blood, medulla oblongata, and thyroid tissues were collected for further testing.

### Thyroid function test

We measured total thyroxine (TT<sub>4</sub>), free thyroxine (FT<sub>4</sub>), and TRAb concentrations in the mouse serum with a commercially available TT<sub>4</sub> and FT<sub>4</sub> radioimmunoassay kit (Cisbio Bioassays, France) and a commercially available TRAb kit (Cisbio Bioassays, France) with a radioimmunoassay  $\gamma$ counter (DFM-96, Zhongcheng Electromechanical Technology Development Co., Ltd., Hefei, China). The normal ranges of TT<sub>4</sub>, FT<sub>4</sub>, and TRAb concentrations were defined as the mean  $\pm$ 3 SD of Ad-Control mice (14).

### Detection of TSHR on vascular endothelial cells of medulla oblongata tissues by immunofluorescence

Gradient xylene was applied to remove the paraffin from the medulla oblongata tissue sections, and then gradient ethanol was used to dehydrate the tissue sections. The endogenous peroxidase was blocked via 3% H<sub>2</sub>O<sub>2</sub>. EDTA antigen retrieval buffer (pH 8.0) was employed to denature the protein and release the antigen. The nonspecific binding was sealed by 30 minutes of incubation with 3% BSA at room temperature. The primary antibody dilution was 1:100 for CD31 (Servicebio, China) and TSHR (Biorbyt #orb247628, UK), the slides were incubated overnight at 4°C. For fluorescence labeling and colocalization, the FITC-HRP and CY3-conjugated secondary antibodies (Servicebio, China) were utilized. 4', 6-diamidino-2-phenylindole was adopted to detect nuclei (DAPI). Microscopy detection and image acquisition were performed by fluorescence microscopy (NIKON Eclipse Ti, Japan). ImageJ software version 1.8.0 was used to examine the degree of TSHR colocalization on vascular endothelial cells.

### Cell cultures

The bEnd.3 cells were obtained from China's Academy of Sciences Type Culture Collection (Shanghai, China). A Dulbecco's modified Eagle's medium (Gibco, USA) containing 10% foetal bovine serum (Gibco, USA), 100 U/ml penicillin, and 100 g/ml streptomycin (Solarbio, China) was used to raise bEnd.3 cells in this study. The cultures were kept at 37°C in a humidified incubator with 5% CO<sub>2</sub> until the end of the experiment. When 3 cells achieved 70% confluence, they were treated with M22 (RSR, #M22/FD/0.04, UK) at 0ng/mL, 5ng/mL, 10ng/mL or 20ng/mL for 24 hours.

### Western blotting

To extract total protein, RIPA lysis solution containing

protease and phosphatase inhibitors was used to lyse medulla oblongata tissue and bEnd.3 cell samples for 30 minutes. Electrophoresis was used to separate equal amounts of protein on 10% SDS-PAGE gels, which were then transferred to PVDF membranes (Millipore, USA). Anti-TSHR antibody (Biorbyt, #orb247628, UK) was treated with the membranes in Tris-buffered saline (TBST) mixed with 5% powdered milk or 5% bovine serum albumin before being incubated with an appropriate secondary antibody. GAPDH was used to normalize the results.

### Real-time fluorescence quantitative PCR (RT-qPCR)

Total RNA was isolated with NucleoZOL RNA extraction reagent (MACHEREY-NAGEL, Germany) and reverse-transcribed into cDNA using a PrimeScript™ RT Master Mix kit (TAKARA, Japan) according to the manufacturer's instructions. RT-qPCR was carried out with a TB Green® Premix Ex Taq™ II kit (TAKARA, Japan), and an ABI7500 Prism real-time PCR equipment, and software (Applied Biosystems, USA). The total reaction volume of 20  $\mu$ l included 500 ng of cDNA as the template. Sangon Biotechnology Co., Ltd. produced primers for GAPDH and TSHR with the following sequences (5'-3'): GAPDH, forward GGTGTCTCCTGCGACTTCA, reverse TGGTCCAGGGTTTCTTACTCC; and TSHR, forward GGTCCTGCTGCTGCTTGTTT, reverse ACTCTGAAGTCGTCCTCCTGGTG. Stage 1: 95°C for 30 seconds; Stage 2: 95°C for 5 seconds and 60°C for 34 seconds (40 cycles); and Stage 3: 95°C for 15 seconds, 60°C for one minute, and 95°C for 15 seconds. To quantify relative mRNA expression, the 2<sup>- $\Delta\Delta$ Ct</sup> technique was utilized (15).

### Detection of TSHR on bEnd.3 cells by immunofluorescence

bEnd.3 cells were grown for 24 hours in a confocal dish (Biosharp, China). The cultures were kept at 37°C in a humidified incubator containing 5% CO<sub>2</sub> until the bEnd.3 cells were treated with M22 (RSR, #M22/FD/0.04, UK) at concentrations of 0ng/mL, 5ng/mL, 10ng/mL, or 20ng/mL for 24 hours after reaching 70% confluence on the top plate of the culture flask. The cells were fixed with 4% paraformaldehyde for 30 minutes, permeabilized in PBS containing 0.1% Triton X-100 for 30 minutes, and then incubated for 2 hours at room temperature in the dark with phalloidin staining reagent (1:200). After blocking with 3% BSA for 30 minutes, the samples were incubated overnight at 4°C with an anti-TSHR primary antibody (Biorbyt #orb247662, UK). Instead of the primary antibody, negative control sections were treated in PBS. The cells were then treated for 50 minutes at room temperature with a 1:400 dilution of goat anti-rabbit secondary antibody. The nuclei were stained with DAPI for 10 minutes at room temperature in the dark. After three washes with PBS, the cells were sealed with mounting media for observation (Servicebio, Wuhan, China). Pictures of cells were captured by using confocal fluorescence microscopy (NIKON Eclipse Ti, Japan). All pictures were obtained with the same intensity and photodetector gain to enable quantitative comparisons of the relative levels of immunoreactivity between samples.

### Quantification of cAMP

bEnd.3 cells were seeded in a 6-well plate and grown to

confluence. The cells were preincubated with 100  $\mu\text{mol/l}$  IBMX (MedChemExpress #HY-12318, USA), an inhibitor of cyclic AMP (cAMP) phosphodiesterase, for 1h and then treated with 50  $\mu\text{mol/l}$  forskolin (MedChemExpress #HY-15371, USA), an adenylyl cyclase activator, or 0ng/mL, 5ng/mL, 10ng/mL, or 20ng/mL M22 for 1 h. The treated cells were lysed in 200  $\mu\text{l}$  of lysis buffer (Solarbio #R0010-100, China) containing 1:1000 phenylmethane-sulfonyl fluoride (PMSF) for 10 minutes, after which they were withdrawn from the culture plate and dissociated using a pipette. The cAMP content of the supernatants was determined using a cAMP ELISA kit (CloudClone #SE-C419Hu, China) according to the manufacturer's instructions following centrifugation at 12000 rpm for 5 minutes.

### Statistical analysis

Graphs were created using version 6.0 of the GraphPad Prism software (GraphPad Software, Inc.). The findings are provided as the mean standard deviation and were analyzed with version 22.0 of the SPSS program (SPSS, Inc.). To analyze differences between groups, a one-way ANOVA was employed.  $p < 0.05$  was determined to be statistically significant.

## Results

### Female BALB/c mouse GD model induced by Ad-TSHR289

There were no significant differences in serum  $\text{TT}_4$ ,  $\text{FT}_4$ , or TRAb levels between the Ad-Control and control groups after female BALB/c mice were inoculated with Ad-TSHR289. The levels of  $\text{TT}_4$ ,  $\text{FT}_4$ , and TRAbs in the Ad-TSHR289 group were all increased than those in the control group and were significantly higher than the mean values in the Ad-Control group  $\pm 3$  SD ( $p < 0.01$ ) (Figure 1). The thyroid of mice in the Ad-TSHR289 group was hyperaemic (Figure 2), compared to that of mice in the control or Ad-Control groups. Haematoxylin and eosin (HE) staining revealed that the thyroid gland of the Ad-TSHR289 group mice shows diffuse hypercellularity and follicles with uneven diameters when compared to normal tissue. Note that the colloid content in the follicular cavity was reduced, the papillary folds protruded into the follicular cavity in hyperplastic thyroid follicles, and no lymphocyte infiltration was found (Figure 2). The size of thyroid follicles in the control and Ad-Control groups was uniform, the arrangement of cells was loose, the epithelial

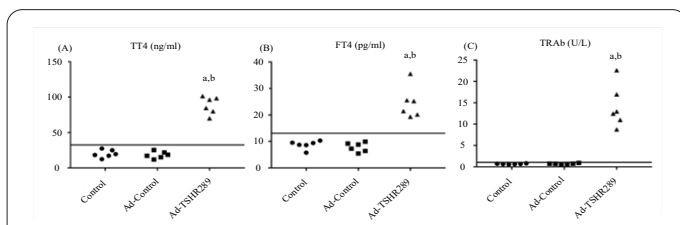


**Figure 1.** Serum total thyroxine (TT4), free thyroxine (FT4) and TRAb levels. TT4 (A), FT4 (B) and TRAb (C) levels were measured 3 weeks after the last immunisation. BALB/c mice were injected with PBS (Control), null adenovirus (Ad-Control), or Ad-TSHR289 adenovirus (Ad-TSHR289). The area below the horizontal lines indicates the mean  $\pm 3$  SD of TT4, FT4 and TRAb values for 6 mice in the Ad-Control group. Significant differences: <sup>a</sup>Control vs. Ad-TSHR289, <sup>b</sup>Ad-Control vs. Ad-TSHR289.

cells in follicles were low cubic or flat, and the content of colloids in follicles was abundant.

### Expression of TSHR in the mouse medulla oblongata

To assess the expression of TSHR in the medulla oblongata of mice, we used RT-qPCR and Western blotting to detect the mRNA and protein expression of TSHR in the medulla oblongata of mice in the control group, the Ad-Control group, and the Ad-TSHR289 group. RT-qPCR and Western blot data indicated that TSHR was expressed normally in the medulla oblongata of all three groups. The relative mRNA and protein expression of TSHR in the medulla oblongata of the Ad-TSHR289 group was significantly higher than that of the control group and the Ad-Control group ( $p < 0.01$ ). (Figures 3 and 4).

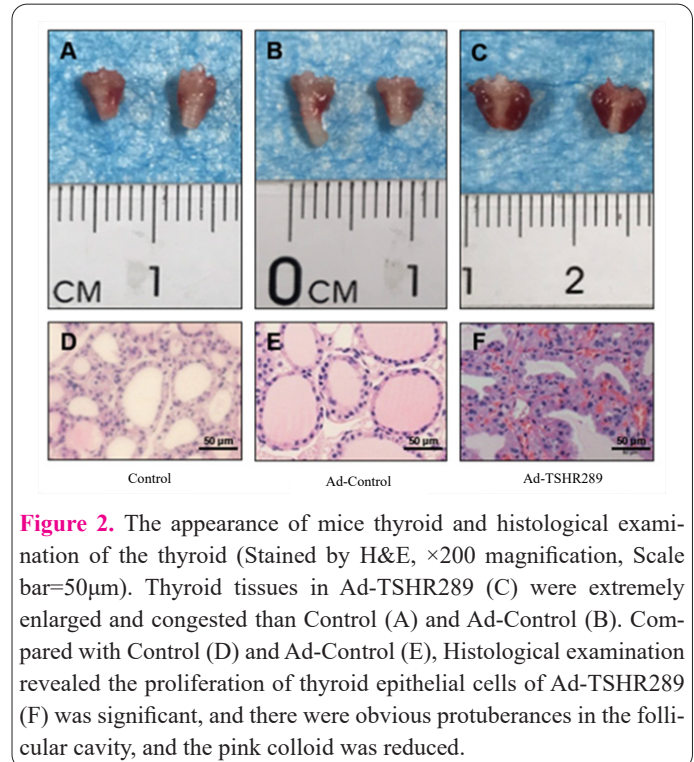


**Figure 2.** The appearance of mice thyroid and histological examination of the thyroid (Stained by H&E,  $\times 200$  magnification, Scale bar = 50  $\mu\text{m}$ ). Thyroid tissues in Ad-TSHR289 (C) were extremely enlarged and congested than Control (A) and Ad-Control (B). Compared with Control (D) and Ad-Control (E), Histological examination revealed the proliferation of thyroid epithelial cells of Ad-TSHR289 (F) was significant, and there were obvious protuberances in the follicular cavity, and the pink colloid was reduced.

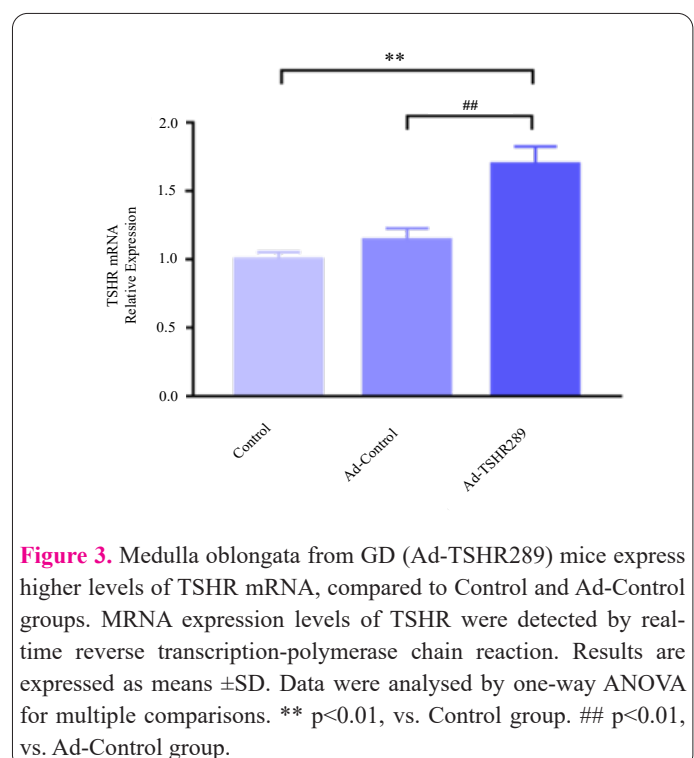


**Figure 3.** Medulla oblongata from GD (Ad-TSHR289) mice express higher levels of TSHR mRNA, compared to Control and Ad-Control groups. MRNA expression levels of TSHR were detected by real-time reverse transcription-polymerase chain reaction. Results are expressed as means  $\pm$  SD. Data were analysed by one-way ANOVA for multiple comparisons. \*\*  $p < 0.01$ , vs. Control group. ##  $p < 0.01$ , vs. Ad-Control group.

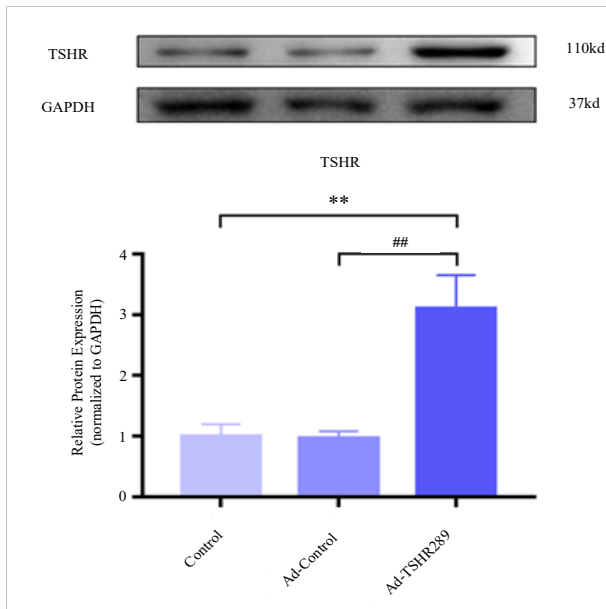


**Figure 4.** Medulla oblongata from GD(Ad-TSHR289) mice express higher levels of TSHR protein, compared to Control and Ad-Control groups. Protein expression levels of TSHR were detected by Western blotting. Results are expressed as means  $\pm$  SD. Data were analysed by one-way ANOVA for multiple comparisons. \*\*  $p < 0.01$ , vs. Control group. ##  $p < 0.01$ , vs. Ad-Control group.

### Fluorescence colocalization of TSHR in vascular endothelial cells in the mouse medulla oblongata

To further clarify the distribution of TSHR in vascular endothelial cells in the mouse medulla oblongata, we used an immunofluorescence homologous double-labelling experiment to examine the expression of TSHR in vascular endothelial cells in the mouse medulla oblongata. CD31 was used as a vascular endothelial marker, the results showed that TSHR-CY3 red staining could be detected in many (but not all) CD31-positive cells in the medulla oblongata in the control group, Ad-Control group and Ad-TSHR289 group, indicating the expression of the TSHR protein in medulla oblongata vascular endothelial cells. The expression of TSHR in the medulla oblongata was increased in the Ad-TSHR289 group compared with the control group and Ad-Control group (Figure 5). Furthermore, the results of the homologous double-labelling experiment were analysed by using Image J software to evaluate the degree of colocalization between TSHR and CD31. The white area was identified as the colocalization overlap region between CD31-positive vascular endothelial cells (FITC, green) and TSHR (CY3, red). The results showed that the area of colocalization overlap for green and red signals in the medulla oblongata in the Ad-TSHR289 group was significantly higher than that in the control group and Ad-Control group, indicating that the expression of TSHR in the medulla oblongata vascular endothelial cells in GD mice was upregulated (Figure 5).

### M22 enhances TSHR expression on the surface of bEnd.3 cells

To confirm whether the difference in TSHR expression on vascular endothelial cells in the medulla oblongata is related to TRAbs, we used 4 different concentrations of M22 to simulate the effect of thyroid-stimulating autoantibodies on bEnd.3 cells in vitro. The mRNA and protein

expression of TSHR in bEnd.3 cells in the different groups were detected by RT-qPCR, Western blot and immunofluorescence assays. The results of the RT-qPCR and Western blot experiments showed that TSHR was normally expressed in the 4 groups of bEnd.3 cells were treated with different concentrations. Compared with that in the 0ng/mL group, the relative mRNA and protein expression of TSHR in the bEnd.3 cell groups treated with M22 were significantly higher ( $p < 0.01$ ) (Figures 6 and 7). In the cell immunofluorescence staining experiment, except for in the negative control group, the distribution of green fluorescence on the cell surface could be seen on bEnd.3 cells were treated with an anti-TSHR primary antibody and a FITC-labelled second antibody. The green signal intensity on the surface of bEnd.3 cells gradually increased with increasing M22 concentrations in the culture medium (Figure 8), indicating that M22 could promote the expression of TSHR on the surface of bEnd.3 cells in vitro and the promotive effect was related to the increase in M22 concentration.

### Detection of the functional activity of TSHR of bEnd.3 cells

Because TSHR can stimulate cAMP production by activating adenylate cyclase after being activated by its ligand, we used an ELISA method to detect the change in the cAMP content of bEnd.3 cells were stimulated with different concentrations of M22 to evaluate the functional activity of TSHR. As shown in Figure 9, compared with that in the control group, the intracellular cAMP content in cells in the M22 treatment groups was increased by 1.28, 1.69 and 2.38 times ( $p < 0.01$ ). However, the production of cAMP in cells treated with IBMX only was slightly increased, and there was no significant difference between

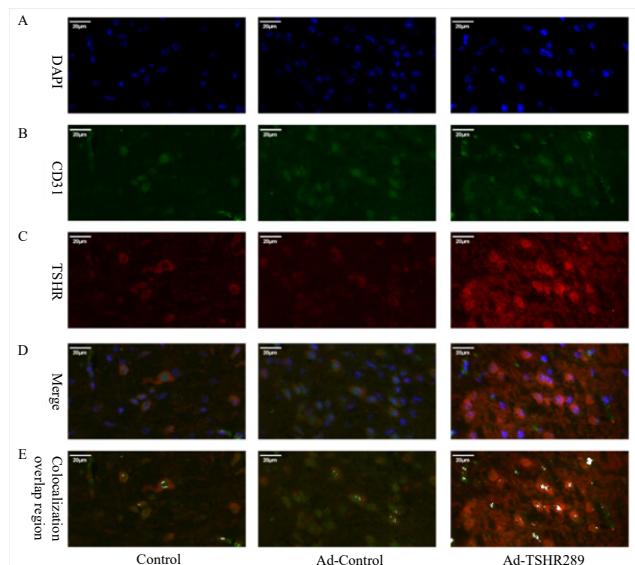


**Figure 5.** Immunofluorescence double staining of mice' medulla oblongata using antibodies against CD31 (FITC, green) and TSHR (CY3, red). The white area was identified as the colocalization overlap region between CD31-positive vascular endothelial cells and TSHR. Colocalization of CD31 and TSHR was observed in the medulla oblongata samples in the control group, Ad-Control group and Ad-TSHR289 group (D). The expression of TSHR in the vascular endothelial cells was increased in the medulla oblongata of the Ad-TSHR289 group compared with the control group and Ad-Control group (E). ( $\times 600$  magnification; Scale bar=20 $\mu$ m).

Discussion

TSHR is a key factor in the regulation of thyroid function and belongs to the G protein-coupled receptor superfamily, which is mainly distributed on the membrane of thyroid follicular epithelial cells (16-18). Under physiological and pathological conditions, ligands such as TSH and TRAbs bind to the extracellular region of TSHR on the surface of thyroid cells, and molecular signals are transmitted to downstream effectors through the hinge and transmembrane regions, thus regulating the proliferation

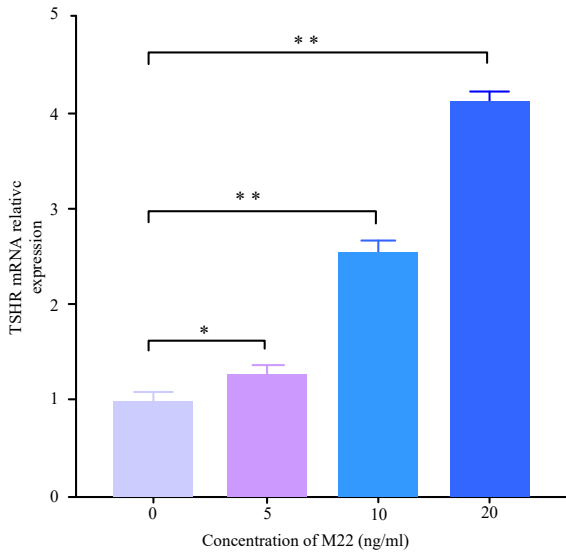


**Figure 6.** Treatment with M22 enhances the expression of TSHR at the mRNA level in bEnd.3 cells. The cells were treated with M22 for 24 h at the indicated concentration. The mRNA levels of TSHR were analyzed by real-time reverse transcription-polymerase chain reaction. Results are expressed as means ± SD. Data were analysed by one-way ANOVA for multiple comparisons. \* p < 0.05, vs. Control group. \*\* p < 0.01, vs. Ad-Control group.

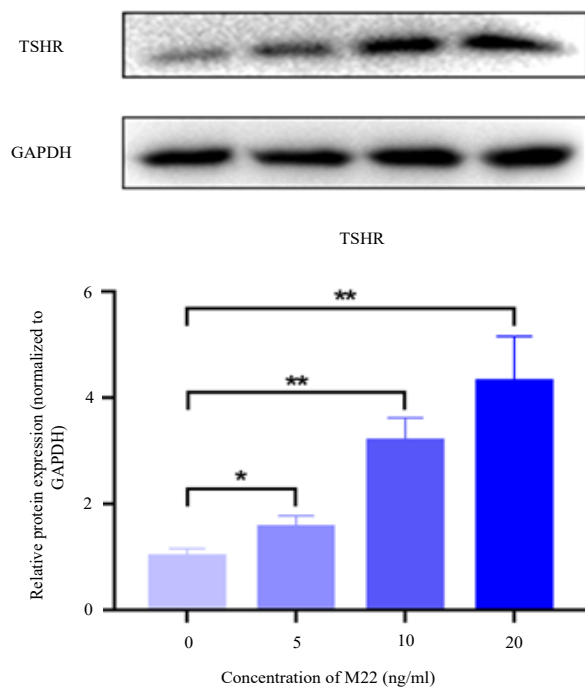


**Figure 7.** Treatment with M22 enhances the expression of TSHR at the protein level in bEnd.3 cells. The cells were treated with M22 for 24 h at the indicated concentration. The protein levels of TSHR were analyzed by western blotting. Results are expressed as means ± SD. Data were analysed by one-way ANOVA for multiple comparisons. \* p < 0.05, vs. Control group. \*\* p < 0.01, vs. Ad-Control group.

the IBMX only and control groups (p>0.05). Additionally, the results of multiple comparisons among the 5ng/mL M22 group, 10ng/mL M22 group and 20ng/mL M22 group showed that there were significant differences in the intracellular cAMP content among the three groups. The above results demonstrated that M22 enhanced the concentration of cAMP in bEnd.3 cells dose-dependently.

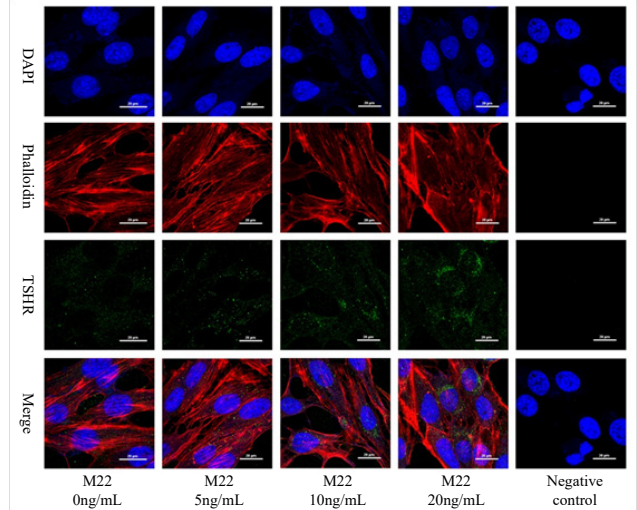


**Figure 8.** Treatment with M22 enhances the expression of TSHR on the surface of bEnd.3 cells. The cells were treated with M22 for 24 h at the indicated concentration. The level of expression of TSHR on the surface of bEnd.3 cells were determined by immunofluorescence. (×600 magnification; Scale bar=20μm).

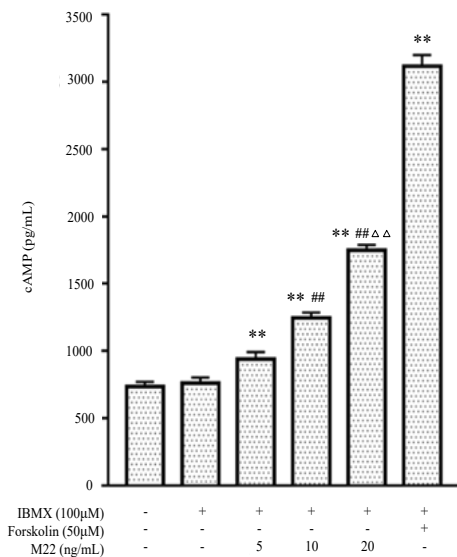


**Figure 9.** Treatment with M22 enhances the cAMP production in bEnd.3 cells. BEnd.3 cells were pretreated with 100 μmol/L IBMX, for 1 h and then treated with forskolin, an adenylyl cyclase activator, or 0ng/mL, 5ng/mL, 10ng/mL, or 20ng/mL M22 for 1 h. The level of cAMP was measured using a cAMP ELISA kit. \*\*p<0.01, vs. control group. ## p<0.01, vs. 5ng/mL group. Δ p<0.01 vs. 10ng/mL group. There was no significant difference between the IBMX only and control groups (p>0.05). Data are expressed as the mean ± SEM of six different groups.

of thyroid follicular epithelial cells and the synthesis and secretion of thyroid hormones (19). As an important thyroid-specific susceptibility gene associated with GD (20), Since it was first cloned in 1989 (21), the structure and function of the TSHR gene and protein have been deeply studied and reported. Although the main role of TSHR is the regulation of thyroid function, its expression is not limited to the thyroid (12). Osteocytes (22), hepatocytes (23), adipocytes (24), retroocular fibroblasts (25), and the central nervous system (26-29) are among the non-thyroid tissues where TSHR is abundantly expressed. These studies discussed and expounded the roles and functions of TSHR in specific tissues and cells of the central nervous system, as well as the associations between the expression of TSHR and the occurrence and development of related diseases, from multiple angles. However, to date, data on the expression and functional characteristics of TSHR in medulla oblongata vascular tissue have not been reported. In this study, we used fluorescence quantitative RT-qPCR, Western blot and immunofluorescence techniques to confirm the expression of TSHR in the local medulla oblongata and cerebral vascular endothelial cells at the mRNA or protein level. Therefore, our results provide more complete evidence for the expression and distribution of TSHR in non-thyroid tissues of mice, especially in the medulla oblongata in the central nervous system. In addition, the ELISA results showed that the TSHR protein expressed in bEnd.3 cells could be recognized by M22 and subsequently increase the level of intracellular cAMP, which confirmed that bEnd.3 cells expressed functional TSHR. This finding makes it possible to further explore the factors related to autoimmune thyroid diseases, especially the involvement of TRAbs in the regulation of cerebrovascular endothelial cell function.

Interestingly, our *in vivo* and *in vitro* results showed not only that TSHR was expressed in the mouse medulla oblongata and cerebrovascular endothelial cells but also that the expression of TSHR in cerebrovascular endothelial cells seemed to be affected by TRAbs. A dose-dependent uptick in mRNA and protein expression of the thyroid-stimulating antibodies (TSAbs) was observed when they were added to cells from patients with hypothyroidism (bEnd3.3). Similar to our results, Jang et al. (30) showed that high-dose M22 could upregulate the gene expression of TSHR in human primary thyroid cells, showing a typical monophasic dose-response curve. This study noted that although TAbs and TSH are both ligands of TSHR, they can continuously activate TSHR on thyroid cells to induce sustained secretion of thyroid hormones. However, as a physiological regulator of TSHR activation, TSH is essentially different from pathophysiological stimulatory TAbs. Therefore, in the regulation of TSHR expression, TSH shows a self-inhibitory protective mechanism against overstimulation of thyroid hormones, while TAbs have the opposite effect. At present, it is not clear why TAbs or M22 promotes increased expression of TSHR in our study. However, TSHR expression in the thyroid gland is regulated by TSH, and this has been documented (31). In addition, thyroid transcription factor-1 (TTF-1) can regulate the expression of TSHR by binding to the smallest promoter of the TSHR gene and transactivating this promoter to realize its biological function (32). Because TTF-1 plays an important role in brain development (33,34), TTF-1 may be involved in the regulation of TSHR expres-

sion in cerebrovascular endothelial cells. But, the regulatory mechanism of TSHR expression needs to be further investigated.

Furthermore, it is worth paying attention to whether the expression of TSHR in a brain region increases or decreases, and the effects of a change in TSHR expression on normal brain development, the maintenance of brain function (35-37), and even the integrity of the blood-brain barrier during some neuropathological diseases (38) have been reported. Furthermore, after TSABs attach to the extracellular domain of TSHR in thyroid cells, they continue to stimulate the TSHR downstream signaling pathway, which can have a variety of physiologic effects (39,40). Considering that TRAbs are an important pathogenic factor in the blood circulation of ATM patients, combined with the correlations between the clinical characteristics of ATM and medulla oblongata lesions mentioned earlier (6,7), the combination of the high concentration of TRAbs and upregulated TSHR expression in ATM patients may indicate important neuropathological interactions in medulla oblongata tissue, especially in medulla oblongata paralysis.

Taken together, our findings show that TRAbs increase the expression of functional TSHR on the surface of medulla oblongata vascular endothelial cells *in vivo* and *in vitro*, in addition to confirming the expression of TSHR in the medulla oblongata and vascular endothelial cells of the brain. The results presented here offer new clues for the study of the mechanism of medulla oblongata dysfunction in ATM.

#### Acknowledgments

We would like to acknowledge the support of the National Key Clinical Specialty Programs (General Surgery & Oncology) and the Key Laboratory of Early Prevention & Treatment for Regional High-Incidence-Tumor (Guangxi Medical University), Ministry of Education, China. As well as the present study is also partly supported by the Research Institute of Innovative Think-tank at Guangxi Medical University (The gene-environment interaction in hepatocarcinogenesis is in Guangxi HCCs and its translational applications in the HCC prevention).

#### Funding

The research is supported by: The National Natural Science Foundation of China, the effect of TRAb on cerebrovascular endothelial cell function and a further integrated research with proteomics and transcriptomics on rat medulla of Graves disease, (No. 81660138); National Natural Science Foundation of China, Research on brain activity changes and molecular mechanism of acute thyrotoxic myopathy based on rest-stating functional magnetic resonance imaging, (No. 81860146).

#### Disclosure

The authors declare that they have no competing interests.

#### References

1. Laurent LPE. Acute thyrotoxic bulbar palsy. *The Lancet* 1944; 243(6281): 87-88. [https://doi.org/10.1016/S0140-6736\(00\)42522-5](https://doi.org/10.1016/S0140-6736(00)42522-5)
2. Bertola G, Ausenda C, Bocchia M, Grassi F, Ciani M, Sassi L. Paralisi della muscolatura bulbare associata a tetraparesi flaccida in

- corso di tireotossicosi [Bulbar paralysis and flaccid tetraparesis in thyrotoxicosis]. *Recenti Prog Med* 2002 ;93(3): 169-171. Italian.
3. Cui H, Zhang X. Thyrotoxic myopathy: research status, diagnosis, and treatment. *Endokrynol Pol* 2022; 73(1) :157-162.
  4. Parperis K, Dadu R, Hoq S, Argento V. Thyrotoxic Dysphagia in an 82-year-old male. *Case Rep Med* 2011; 2011: 929523. <https://doi.org/10.1155/2011/929523>
  5. Boddu NJ, Badireddi S, Straub KD, Schwankhaus J, Jagana R. Acute thyrotoxic bulbar myopathy with encephalopathic behaviour: an uncommon complication of hyperthyroidism. *Case Rep Endocrinol* 2013; 2013: 369807. <https://doi.org/10.1155/2013/369807>
  6. Ramsay I. Thyrotoxic muscle disease. *Postgrad Med J* 1968; 44(511): 385-397. <https://doi.org/10.1136/pgmj.44.511.385>
  7. Chapman EM, Maloof F. Bizarre clinical manifestations of hyperthyroidism. *N Engl J Med* 1956; 254(1): 1-5. <https://doi.org/10.1056/NEJM195601052540101>
  8. Smith TJ, Hegedüs L. Graves' Disease. *N Engl J Med* 2016; 375(16): 1552-1565. <https://doi.org/10.1056/NEJMra1510030>
  9. Smith BR, Sanders J, Furmaniak J. TSH receptor antibodies. *Thyroid*. 2007; 17(10): 923-938. <https://doi.org/10.1089/thy.2007.0239>
  10. Sanders J, Miguel RN, Furmaniak J, Smith BR. TSH receptor monoclonal antibodies with agonist, antagonist, and inverse agonist activities. *Methods Enzymol* 2010; 485: 393-420. <https://doi.org/10.1016/B978-0-12-381296-4.00022-1>
  11. McLachlan SM, Rapoport B. Breaking tolerance to thyroid antigens: changing concepts in thyroid autoimmunity. *Endocr Rev* 2014; 35(1): 59-105. <https://doi.org/10.1210/er.2013-1055>
  12. Williams GR. Extrathyroidal expression of TSH receptor. *Ann Endocrinol (Paris)* 2011; 72(2): 68-73. <https://doi.org/10.1016/j.ando.2011.03.006>
  13. Liu L, Wu L, Gao A, Zhang Q, Lv H, Xu L, Xie C, Wu Q, Hou P, Shi B. The Influence of Dihydrotestosterone on the Development of Graves' Disease in Female BALB/c Mice. *Thyroid* 2016; 26(3): 449-457. <https://doi.org/10.1089/thy.2015.0620>
  14. Tang Y, Zhu X, Feng H, Zhu L, Fu S, Kong B, Liu X. An improved mouse model of Graves disease by once immunization with Ad-TSHR289. *Endocr J* 2019; 66(9): 827-835. <https://doi.org/10.1507/endocrj.EJ19-0148>
  15. Livak KJ, Schmittgen TD. Analysis of relative gene expression data using real-time quantitative PCR and the 2(-Delta Delta C(T)) Method. *Methods* 2001; 25(4): 402-408. <https://doi.org/10.1006/meth.2001.1262>
  16. Paschke R, Ludgate M. The thyrotropin receptor in thyroid diseases. *N Engl J Med* 1997; 337(23): 1675-1681. <https://doi.org/10.1056/NEJM199712043372307>
  17. Fredriksson R, Lagerström MC, Lundin LG, Schiöth HB. The G-protein-coupled receptors in the human genome form five main families. Phylogenetic analysis, paralogon groups, and fingerprints. *Mol Pharmacol* 2003; 63(6): 1256-1272. <https://doi.org/10.1124/mol.63.6.1256>
  18. Davies TF, Yin X, Latif R. The genetics of the thyroid stimulating hormone receptor: history and relevance. *Thyroid* 2010; 20(7): 727-736. <https://doi.org/10.1089/thy.2010.1638>
  19. Rapoport B, Chazenbalk GD, Jaume JC, McLachlan SM. The thyrotropin (TSH) receptor: interaction with TSH and autoantibodies. *Endocr Rev* 1998; 19(6): 673-716. <https://doi.org/10.1210/edrv.19.6.0352>
  20. Lee HJ, Li CW, Hammerstad SS, Stefan M, Tomer Y. Immunogenetics of autoimmune thyroid diseases: A comprehensive review. *J Autoimmun* 2015; 64: 82-90. <https://doi.org/10.1016/j.jaut.2015.07.009>
  21. Parmentier M, Libert F, Maenhaut C, Lefort A, Gérard C, Perret J, Van Sande J, Dumont JE, Vassart G. Molecular cloning of the thyrotropin receptor. *Science* 1989; 246(4937): 1620-1622. <https://doi.org/10.1126/science.2556796>
  22. Abe E, Marians RC, Yu W, Wu XB, Ando T, Li Y, Iqbal J, Eldeiry L, Rajendren G, Blair HC, Davies TF, Zaidi M. TSH is a negative regulator of skeletal remodeling. *Cell* 2003; 115(2): 151-162. [https://doi.org/10.1016/s0092-8674\(03\)00771-2](https://doi.org/10.1016/s0092-8674(03)00771-2)
  23. Zhang W, Tian LM, Han Y, Ma HY, Wang LC, Guo J, Gao L, Zhao JJ. Presence of thyrotropin receptor in hepatocytes: not a case of illegitimate transcription. *J Cell Mol Med* 2009; 13(11-12): 4636-4642. <https://doi.org/10.1111/j.1582-4934.2008.00670.x>
  24. Endo T, Ohta K, Haraguchi K, Onaya T. Cloning and functional expression of a thyrotropin receptor cDNA from rat fat cells. *J Biol Chem* 1995; 270(18): 10833-10837. <https://doi.org/10.1074/jbc.270.18.10833>
  25. Mengistu M, Lukes YG, Nagy EV, Burch HB, Carr FE, Lahiri S, Burman KD. TSH receptor gene expression in retroocular fibroblasts. *J Endocrinol Invest* 1994; 17(6): 437-441. <https://doi.org/10.1007/BF03347732>
  26. Bockmann J, Winter C, Wittkowski W, Kreutz MR, Böckers TM. Cloning and expression of a brain-derived TSH receptor. *Biochem Biophys Res Commun* 1997; 238(1): 173-178. <https://doi.org/10.1006/bbrc.1997.7268>
  27. Prummel MF, Brokken LJ, Meduri G, Misrahi M, Bakker O, Wiersinga WM. Expression of the thyroid-stimulating hormone receptor in the folliculo-stellate cells of the human anterior pituitary. *J Clin Endocrinol Metab* 2000; 85(11): 4347-4353. <https://doi.org/10.1210/jcem.85.11.6991>
  28. Crisanti P, Omri B, Hughes E, Meduri G, Hery C, Clauser E, Jacquemin C, Saunier B. The expression of thyrotropin receptor in the brain. *Endocrinology* 2001; 142(2): 812-822. <https://doi.org/10.1210/endo.142.2.7943>
  29. Naicker M, Naidoo S. Expression of thyroid-stimulating hormone receptors and thyroglobulin in limbic regions in the adult human brain. *Metab Brain Dis* 2018; 33(2): 481-489. <https://doi.org/10.1007/s11011-017-0076-3>
  30. Jang D, Morgan SJ, Klubo-Gwiezdzinska J, Banga JP, Neumann S, Gershengorn MC. Thyrotropin, but Not Thyroid-Stimulating Antibodies, Induces Biphasic Regulation of Gene Expression in Human Thyrocytes. *Thyroid* 2020; 30(2): 270-276. <https://doi.org/10.1089/thy.2019.0418>
  31. Saito T, Endo T, Nakazato M, Kogai T, Onaya T. Thyroid-stimulating hormone-induced down-regulation of thyroid transcription factor 1 in rat thyroid FRTL-5 cells. *Endocrinology* 1997; 138(2): 602-606. <https://doi.org/10.1210/endo.138.2.4918>
  32. Civitareale D, Castelli MP, Falasca P, Saiardi A. Thyroid transcription factor 1 activates the promoter of the thyrotropin receptor gene. *Mol Endocrinol* 1993; 7(12): 1589-1595. <https://doi.org/10.1210/mend.7.12.8145764>
  33. Lazzaro D, Price M, de Felice M, Di Lauro R. The transcription factor TTF-1 is expressed at the onset of thyroid and lung morphogenesis and in restricted regions of the foetal brain. *Development* 1991; 113(4): 1093-1104. <https://doi.org/10.1242/dev.113.4.1093>
  34. Bingle CD. Thyroid transcription factor-1. *Int J Biochem Cell Biol* 1997; 29(12): 1471-1473. [https://doi.org/10.1016/s1357-2725\(97\)00007-1](https://doi.org/10.1016/s1357-2725(97)00007-1)
  35. Bradley DJ, Towle HC, Young WS 3rd. Spatial and temporal expression of alpha- and beta-thyroid hormone receptor mRNAs, including the beta 2-subtype, in the developing mammalian nervous system. *J Neurosci* 1992; 12(6): 2288-2302. <https://doi.org/10.1523/JNEUROSCI.12-06-02288.1992>
  36. Bernal J. Thyroid hormone receptors in brain development and function. *Nat Clin Pract Endocrinol Metab* 2007; 3(3): 249-259.

- <https://doi.org/10.1038/ncpendmet0424>
37. Wallis K, Dudazy S, van Hogerlinden M, Nordström K, Mittag J, Vennström B. The thyroid hormone receptor alpha1 protein is expressed in embryonic postmitotic neurons and persists in most adult neurons. *Mol Endocrinol* 2010; 24(10): 1904-1916. <https://doi.org/10.1210/me.2010-0175>
38. Naicker M, Abbai N, Naidoo S. Bipolar limbic expression of auto-immune thyroid targets: thyroglobulin and thyroid-stimulating hormone receptor. *Metab Brain Dis* 2019; 34(5): 1281-1298. <https://doi.org/10.1007/s11011-019-00437-w>
39. Endo T. [Thyrotropin receptor--structure, autoantibody and signal transduction]. *Nihon Rinsho* 2006; 64(12): 2203-2207. Japanese.
40. Morshed SA, Latif R, Davies TF. Characterization of thyrotropin receptor antibody-induced signaling cascades. *Endocrinology* 2009; 150(1): 519-529. <https://doi.org/10.1210/en.2008-0878>